

Charge pumping in carbon nanotube quantum dots

M.R. Buitelaar,¹ V. Kashcheyevs,^{2,3} P.J. Leek,¹ V.I. Talyanskii,¹
C.G. Smith,¹ D. Anderson,¹ G.A.C. Jones,¹ J. Wei,⁴ and D.H. Cobden⁴

¹*Cavendish Laboratory, University of Cambridge, Cambridge, CB3 0HE, UK*

²*Institute for Solid State Physics, University of Latvia, Riga, LV-1063, Latvia*

³*Faculty of Physics and Mathematics, University of Latvia, Riga, LV-1002, Latvia*

⁴*Department of Physics, University of Washington, Seattle, Washington 98195-1560, USA*

(Dated: August 13, 2021)

We investigate charge pumping in carbon nanotube quantum dots driven by the electric field of a surface acoustic wave. We find that at small driving amplitudes, the pumped current reverses polarity as the conductance is tuned through a Coulomb blockade peak using a gate electrode. We study the behavior as a function of wave amplitude, frequency and direction and develop a model in which our results can be understood as resulting from adiabatic charge redistribution between the leads and quantum dots on the nanotube.

PACS numbers: 73.63.Kv, 73.23.Hk, 73.63.Fg, 85.35.Kt, 72.50.+b

The dynamics of charge transport at the level of single electrons or electron spins in nanoscale systems such as quantum dots is important from both applied and fundamental viewpoints. A sensitive probe of the response of a quantum dot to changing external parameters (e.g. a gate voltage or magnetic field) is the dc charge pumping current generated in the absence of an applied bias [1]. A general result for open, non-interacting electron systems is the Brouwer formula which relates the pumped current to the scattering matrix of the system [2]. In interacting systems, correlations add complexity and modify the predictions. Recent theoretical work has considered pumping in quantum dots with weak interactions [3, 4], in the Kondo regime [5], in the Coulomb blockade regime [6], and for superconducting leads [7, 8]. For the case of interacting electrons in one dimension (the Luttinger liquid), current quantization [9, 10] and pure spin currents [11] have been predicted.

Experimentally, the rich variety of predicted phenomena has remained largely unexplored [12, 13]. A promising system to test the various theories of charge pumping is carbon nanotubes, since all of the transport regimes mentioned above have already been realized in conventional nanotube devices [14, 15, 16]. In this Letter we pursue the potential of nanotubes, demonstrating charge pumping in nanotube quantum dots up to frequencies of 2.6 GHz and present a theoretical description of the observed effects.

While charge pumping could in principle be realized by modulating side or top gates that are capacitively coupled to the nanotubes [17], we adopt a different approach in which a surface acoustic wave (SAW) pumps charge through a carbon nanotube [18, 19, 20, 21]. An individual nanotube is contacted on a piezoelectric quartz substrate by palladium source and drain electrode that are separated by 5 μm (Fig. 1(c) lower right inset). A side gate electrode is used to vary the electrostatic potential in the nanotube. Several mm beyond each contact are two SAW transducers (Fig. 1(c) left inset) having resonant frequencies f_{SAW} of about 2.6 GHz and 544 MHz. The electric

field accompanying the SAW pumps charge through the nanotube. While the use of SAWs restricts experiments to the transducers' resonant frequencies, it avoids direct capacitive coupling between the high-frequency and device electrodes and enables a clear distinction between the signal due to the SAW (possible only at the transducers' resonant frequencies) and rectified currents from radiated fields (possible at all frequencies). Details of sample fabrication, transducer operation and propagating SAW fields were described in Ref. [19].

Fig. 1(a) shows the dc transport properties of the nanotube at temperature $T = 5$ K. The approximate periodicity and large charging energy $U_C \sim 10 - 15$ meV observed indicate that the nanotube is divided into two (or more) sections such that the conductance is dominated by Coulomb blockade of a single electron puddle that is much smaller than the 5 μm source-drain separation. This also follows from the suppression of the linear-response conductance and additional features (arrows) observed in the differential conductance (see inset to Fig. 1(a)) [22]. Fig. 1(c) shows the induced current, I_{SAW} , in the presence of a SAW field at 2607 MHz in the absence of a source-drain bias voltage. For a SAW velocity $v_{\text{SAW}} \approx 3200$ m/s on quartz this corresponds to a SAW wavelength $\lambda_{\text{SAW}} = v_{\text{SAW}}/f_{\text{SAW}} \sim 1.2$ μm [19]. When a low power P_{SAW} is applied to the SAW transducers, a dc current is induced whose direction alternates as a sensitive function of gate voltage V_g . The peak-and-dip features in the current are clearly correlated with the Coulomb blockade peaks, and the current changes polarity on reversal of the SAW direction.

These features were studied in more detail as a function of SAW amplitude and for both available SAW frequencies. Figure 2(a) shows I_{SAW} as a function of P_{SAW} . The peak-and-dip features increase in magnitude and move outwards as P_{SAW} is increased. When we plot the derivative of the current with respect to the SAW amplitude $V_{\text{SAW}} \propto P_{\text{SAW}}^{1/2}$, as in Fig. 2(c), it becomes apparent that the dominant features move essentially linearly with V_{SAW} . At the highest applied SAW powers (up to 20 dBm

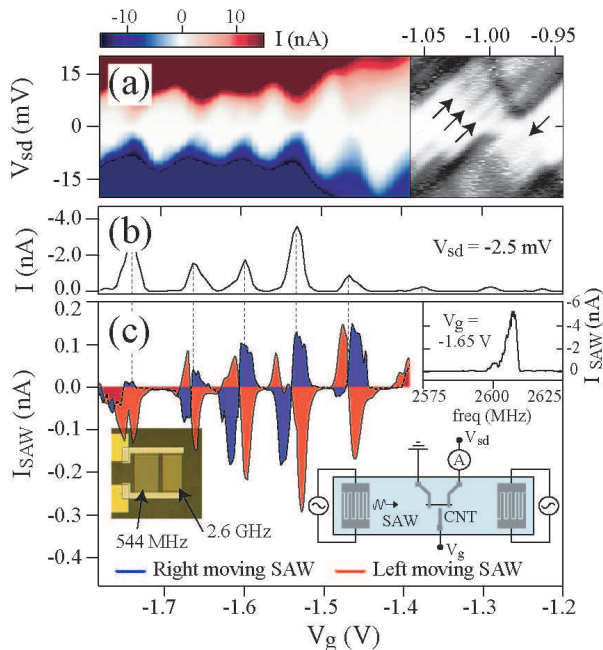


FIG. 1: (a) Color scale representation of the current as a function of V_{sd} and V_g . Inset: differential conductance around a Coulomb peak (dark = more conductive) (b) Current trace at $V_{sd} = -2.5$ mV showing Coulomb blockade oscillations. (c) SAW induced current as a function of V_g in the absence of an applied bias. In red is the current produced by the left-moving SAW at 2602 MHz with $P_{\text{SAW}} = -15$ dBm. In blue is the current produced by the right-moving SAW at 2607 MHz with $P_{\text{SAW}} = -10$ dBm. Right inset: simplified schematic of the device. Left inset: photograph of one of the transducers, which is able to generate SAWs at frequencies of both 2607 MHz and 544 MHz. Top inset: frequency dependence of the current at $V_g = -1.65$ V and $P_{\text{SAW}} = 15$ dBm.

or 100 mW) the features merge into a background of current in the direction of the SAW across the whole gate voltage range [18].

Assuming that the dominant action of the SAW is to modulate the electrostatic potential at the nanotube, we can estimate the actual value of V_{SAW} from the linear evolution of the current features with amplitude and the gate efficiency deduced from the dc Coulomb blockade pattern. We find a SAW amplitude $V_{\text{SAW}} \simeq 150$ mV at the maximum power $P_{\text{SAW}} = 20$ dBm applied to the left transducer. This agrees with estimates from transducer impedance calculations and direct transducer transmittance measurements [19]. The inset to Fig. 1(c) shows I_{SAW} as a function of frequency. A peak is observed at the transducer resonant frequency only, demonstrating that the observed current features do not result from directly radiated fields or from photon-assisted tunneling (see also Refs. [18, 19]).

All the observed behavior can be explained by a model in which disorder in the nanotube causes it to contain two or more localized electron puddles in series. The SAW modulates the energies of the states in these puddles and

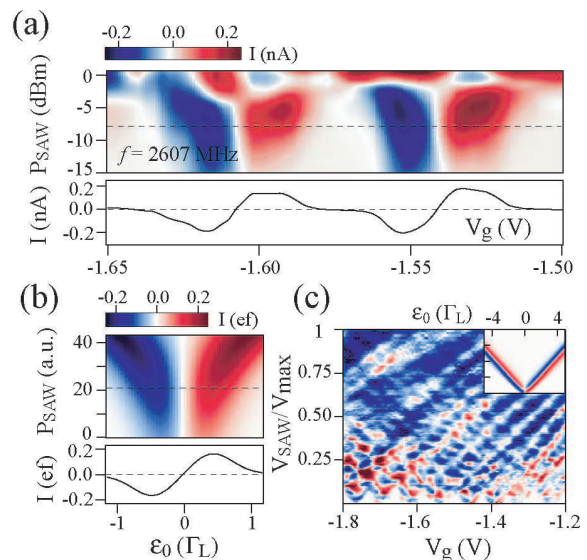


FIG. 2: (a) Color scale representation of the SAW-induced current as function of V_{sd} and V_g , showing sign reversal as V_g crosses a Coulomb blockade peak. The line trace is taken at $P_{\text{SAW}} = -8$ dBm. (b) Calculated current using the model explained in the main text. (c) Derivative of the SAW induced current with respect to the SAW amplitude as a function of V_g and (normalized) V_{SAW} . The maximum SAW amplitude is estimated to be $\sim 100 - 150$ mV. Inset: dI/dV_{SAW} as calculated in the model, showing the same linear peak splitting.

adiabatic charge redistribution between the puddles and the leads gives rise to a dc current. We first discuss a minimal model in which there are two puddles, each acting as a quantum dot with a single spinless level (see Fig. 3(a)), before introducing asymmetries in the tunnel couplings and multiple levels in the dots to better reflect the likely experimental situation. Such a simple two-level system provides a useful approximation to the Coulomb blockade physics of tunnel-coupled double dots; see e.g. Ref. [23]. The only parameters that enter the model are the tunnel couplings Γ_L and Γ_R of the left and right dots to left and right leads respectively, V_{SAW} , the phase difference ϕ of the SAW between the two dots, and the tunnel coupling Δ between them. The instantaneous effective Hamiltonian of this double-dot system can be written as

$$\mathcal{H}_d = \begin{bmatrix} \varepsilon_1 - i\Gamma_L/2 & \Delta/2 \\ \Delta/2 & \varepsilon_2 - i\Gamma_R/2 \end{bmatrix}. \quad (1)$$

For any periodic time dependence of the dot energies ε_1 and ε_2 , the adiabatic current [2, 24, 25, 26] from left to right can be calculated as a surface integral [2], $I = ef \int_A R(\varepsilon_1, \varepsilon_2) d\varepsilon_1 d\varepsilon_2$, over the area A enclosed parametrically by the pumping trajectory in the $(\varepsilon_1, \varepsilon_2)$ -plane.

The response function R can be obtained from Eq. 1, see e.g. Ref. [26], and in the zero-temperature limit takes

a straightforward form, $R(\varepsilon_1, \varepsilon_2) =$

$$\frac{-(32/\pi)\Delta^2\Gamma_L\Gamma_R(\varepsilon_1\Gamma_R + \varepsilon_2\Gamma_L)}{[2\Gamma_L\Gamma_R\Delta^2 + 4\varepsilon_1^2\Gamma_R^2 + 4\varepsilon_2^2\Gamma_L^2 + (\Delta^2 - 4\varepsilon_1\varepsilon_2)^2 + \Gamma_L^2\Gamma_R^2]^2},$$

The response function is shown graphically in Fig. 3(b,c) for different parameter values. It exhibits one pronounced minimum (blue) and one maximum (red). For the pumping trajectory, we assume the SAW periodically modulates the levels according to

$$\begin{aligned} \varepsilon_1 &= -\delta/2 + \alpha_1 eV_g + eV_{\text{SAW}} \cos(2\pi ft), \\ \varepsilon_2 &= +\delta/2 + \alpha_2 eV_g + eV_{\text{SAW}} \cos(2\pi ft + \phi). \end{aligned} \quad (2)$$

Here α_1 and α_2 are the coupling efficiencies of the gate to the two dots and δ is a level offset parameter. The effect of the SAW on the tunnel barriers is thought to be negligible for the small SAW amplitudes considered here. For the case of symmetric coupling $\Gamma_L = \Gamma_R$ (Fig. 3(b)), we see that the peaks of negative and positive pumping current, as seen in Fig. 2(b) correspond to elliptical trajectories around the two triple points in the stability diagram of the double dot [23, 27]. In obvious notation we may represent these as the $(0,0) \rightarrow (0,1) \rightarrow (1,0) \rightarrow (0,0)$ electron and $(1,1) \rightarrow (0,1) \rightarrow (1,0) \rightarrow (1,1)$ hole cycles, respectively.

One property of the pumping current that follows immediately is that it changes polarity when the direction of the pumping contour reverses, i.e., when the SAW direction is reversed. Another is that for small SAW amplitudes, $I \propto V_{\text{SAW}}^2 \sin \phi$ [2], because in this limit $R(\varepsilon_1, \varepsilon_2)$ is approximately constant within the area $A = \pi e^2 V_{\text{SAW}}^2 \sin \phi$ enclosed by the trajectories.

As V_g is varied, the center of the pumping trajectory follows a straight line which for the simple case $\alpha_1 = \alpha_2$ and $\delta = 0$ is the solid diagonal in Fig. 3(b)-(d). In this case, the current traces $I(V_g)$ exhibit symmetric sign-reversing features. If the dots are single-level and completely symmetric, i.e., $\Gamma_L = \Gamma_R$ and $\delta = 0$, then the current traces for different P_{SAW} are dependent only on the ratio Δ/Γ . This simple situation already matches the experimental data quite well, as shown in Fig. 2(b), taking $\Delta/\Gamma = 0.5$. Figure 3 also illustrates the effects of asymmetries. A nonzero level offset δ shifts the diagonal line [see e.g. the dotted line in Fig. 3(b)], while asymmetric coupling to the gate, $\alpha_1 \neq \alpha_2$, changes the slope (dashed line). The result is an asymmetry between the positive and negative current peaks which is most pronounced in the weak pumping regime. For larger SAW powers, such that $eV_{\text{SAW}} \geq \delta$, the difference between positive and negative peaks begins to average out. In the limit of strong pumping, the pumping trajectories encompass both positive and negative parts of $R(\varepsilon_1, \varepsilon_2)$ whose contributions to the pumping tend to cancel. This explains the experimental observation (Fig. 2(c)) that the opposite-sign peak pairs in the pumping current vs V_g move apart linearly in V_{SAW} : the peak current occurs where the integral of R is maximal as a function of ε_0 , and this occurs at $|\varepsilon_0| \sim eV_{\text{SAW}}$

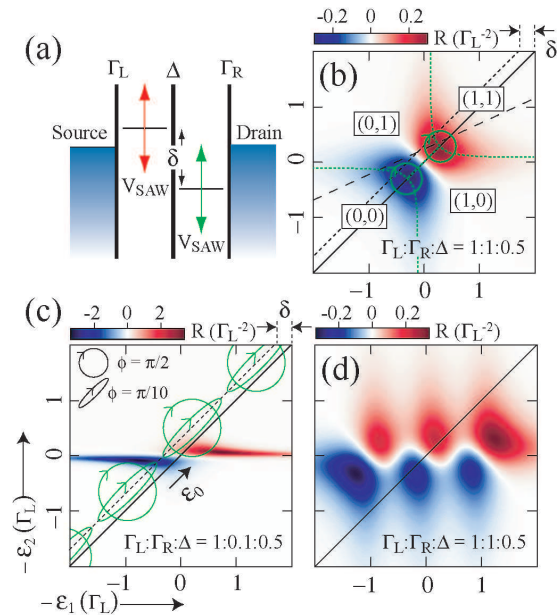


FIG. 3: (a) Schematic of a double dot in which the single-electron states are periodically modulated by the SAW with phase difference ϕ . (b) Color scale representation of the function $R(\varepsilon_1, \varepsilon_2)$ for symmetric coupling to the leads. The SAW-induced current is proportional to the integral of this function over the area traversed in $[\varepsilon_1, \varepsilon_2]$ space. For $\phi = \pi/2$ the trajectories are circles with diameters proportional to V_{SAW} ; for $\phi = \pi/10$ they are narrow ellipses. The ordered pairs (n, m) indicate the electron occupancy of the quantum dots. (c) Same as panel (b) for asymmetric coupling to the leads. The direction ε_0 corresponds to the case of equal coupling of the dots to the gate, $\alpha_1 = \alpha_2$. (d) Calculation of $R(\varepsilon_1, \varepsilon_2)$ with 3 levels on the left dot taken to have spacing equal to 2Δ and identical couplings to the level in the other dot.

The qualitative behavior of the model is quite insensitive to details such as asymmetry in the tunnel couplings or a multiplicity of levels in the dots. In particular the experimental situation in which the conductance is dominated by a single quantum dot can be modelled by taking a single level on the right dot and multiple levels on the left, as shown in Fig. 3(d). The sign-reversing nature of the $I_{\text{SAW}}-V_g$ traces is still a robust feature although signatures of extra levels may appear for certain pumping trajectories [28].

Finally, we examine whether the experimental effects of changing λ_{SAW} are consistent with the model. Fig. 4(a) shows I_{SAW} at $f_{\text{SAW}} = 2607$ MHz in the vicinity of a Coulomb peak. A slight asymmetry between positive and negative peaks is seen for small P_{SAW} . In the model this is reproduced (see Fig. 4(b)) by, for instance, assuming an asymmetric coupling to the leads and a small offset δ , corresponding to the situation depicted in Fig. 3(c). Other kinds of asymmetry such as $\alpha_1 \neq \alpha_2$ have a similar result. Fig. 4(c) shows the current at $f_{\text{SAW}} = 544$ MHz, using the second pair of transducers with larger finger spacing. The current is now nearly always of neg-

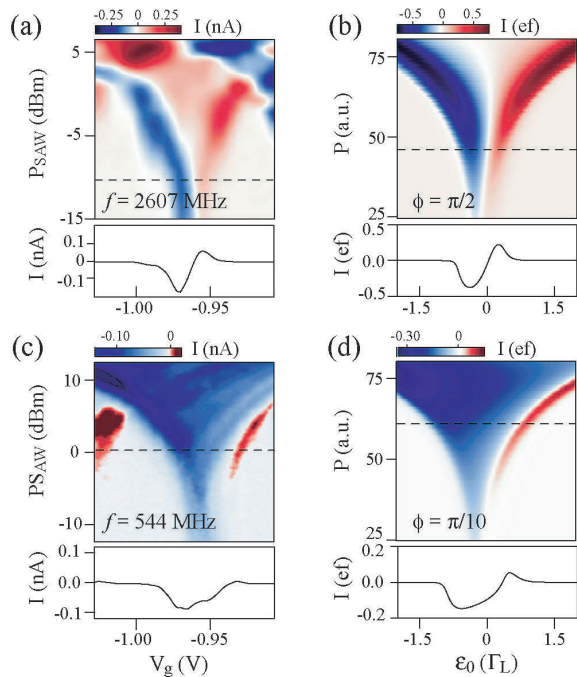


FIG. 4: (a) Color scale representation of the SAW-induced current as a function of SAW power and V_g for $f_{\text{SAW}} = 2607$ MHz. (b) Calculated SAW current for a double QD model with an asymmetry between the tunnel couplings Γ_L and Γ_R , as discussed in the text. The parameters are $\Gamma_L : \Gamma_R : \Delta : \delta = 1.0 : 0.1 : 0.5 : 0.3$, and the phase difference $\phi = \pi/2$. (c) SAW-induced current for the same resonance peak as in panel (a) for $f_{\text{SAW}} = 544$ MHz. (d) Calculated SAW current as in panel (b) but for a phase difference $\phi = \pi/10$ [29]

active polarity. Fig. 4(d) shows the corresponding model prediction, which agrees very well. Here, the effect of decreasing f_{SAW} is just to reduce the phase difference between the dots ($\phi \rightarrow 0$ when λ_{SAW} becomes much larger than the device dimensions). This reduces the width and area of the elliptical pumping trajectory. The result can be understood qualitatively from Fig. 3(c) noting that the level offset δ shifts the line followed by the ellipse center towards the negative (blue) regions of $R(\varepsilon_1, \varepsilon_2)$. For large SAW powers and circular pumping trajectories, the enclosed area includes a domain where $R(\varepsilon_1, \varepsilon_2)$ is positive. However, after decreasing P_{SAW} (smaller radius) or f_{SAW} (narrower ellipse) the integral only includes regions of negative $R(\varepsilon_1, \varepsilon_2)$, enhancing the asymmetry. Note that the enhancement of the asymmetry in I_{SAW} when decreasing SAW power or frequency is expected whenever the center of the pumping trajectory follows a line in $[\varepsilon_1, \varepsilon_2]$ parameter space that is asymmetric with respect to the minima and maxima of $R(\varepsilon_1, \varepsilon_2)$, irrespective of the precise form of this function. The results in Fig. 4 are therefore consistent with the model also when in the experiment $R(\varepsilon_1, \varepsilon_2)$ is significantly more complex than the model situations shown in Fig. 3. To completely describe the experiment (the model actually underestimates the amount of pumped current and does not account for the fine structure observed at 544 MHz) would require a better knowledge of the microscopic details of the device than we have at present.

We thank A. Aharony, O. Entin-Wohlman, and L. Levitov for discussions. MB has been supported by the UK QIP IRC (GR/S82176/01). VK has been supported by Latvian Council of Science, European Social Fund and German-Israeli Project Cooperation (DIP).

-
- [1] D.J. Thouless, Phys. Rev. B **27**, 6083 (1983).
[2] P.W. Brouwer, Phys. Rev. B **58**, R10135 (1998).
[3] I.L. Aleiner and A.V. Andreev, Phys. Rev. Lett. **81**, 1286 (1998).
[4] P.W. Brouwer, A. Lamacraft, and K. Flensberg, Phys. Rev. B **72**, 075316 (2005).
[5] T. Aono, Phys. Rev. Lett. **93**, 116601 (2004).
[6] J. Splettstoesser, M. Governale, J. König, and R. Fazio, Phys. Rev. Lett. **95**, 246803 (2005).
[7] M. Blaauboer, Phys. Rev. B **65**, 235318 (2002).
[8] J. Splettstoesser, M. Governale, J. König, F. Taddei, and R. Fazio, Phys. Rev. B **75**, 235302 (2007).
[9] V.I. Talyanskii, D.S. Novikov, B.D. Simons, and L.S. Levitov, Phys. Rev. Lett. **87**, 276802 (2001).
[10] D.S. Novikov, Phys. Rev. Lett. **95**, 066401 (2005).
[11] R. Citro, N. Andrei, and Q. Niu, Phys. Rev. B **68**, 165312 (2003).
[12] H. Pothier, P. Lafarge, C. Urbina, D. Esteve, and M.H. Devoret, Europhys. Lett. **17**, 249 (1992).
[13] M. Switkes *et al.*, Science **283**, 1905 (1999).
[14] J. Nygård, D.H. Cobden, and P.E. Lindelof, Nature **408**, 342 (2000).
[15] M. Bockrath *et al.*, Nature **397**, 598 (1999).
[16] M.R. Buitelaar *et al.*, Phys. Rev. Lett. **91**, 057005 (2003).
[17] Y. Wei, J. Wang, H. Guo, and C. Roland, Phys. Rev. B **64**, 115321 (2001).
[18] P.J. Leek *et al.*, Phys. Rev. Lett. **95**, 256802 (2005).
[19] M.R. Buitelaar *et al.*, Semicond. Sci. Technol. **21**, S69 (2006).
[20] J. Ebbecke, C.J. Strobl, and A. Wixforth, Phys. Rev. B **70**, 233401 (2004).
[21] Y-S. Shin *et al.*, Phys. Rev. B **74**, 195415 (2006).
[22] The features in the dI/dV are tentatively interpreted as signatures of the charging energy of a second (smaller) quantum dot in series, see e.g. J. Park and P.L. McEuen, Appl. Phys. Lett. **79**, 1361 (2001).
[23] W.G. van der Wiel *et al.*, Rev. Mod. Phys. **75**, 1 (2003).
[24] M. Büttiker, H. Thomas, and A. Prêtre, Z. Phys. B **94**, 133 (1994).
[25] O. Entin-Wohlman, A. Aharony, and Y. Levinson, Phys. Rev. B **65**, 195411 (2002).
[26] V. Kashcheyevs, A. Aharony, and O. Entin-Wohlman, Phys. Rev. B **69**, 195301 (2004).
[27] W.J.M. Naber *et al.*, Phys. Rev. Lett. **96**, 136807 (2006).
[28] This also holds when the level spacing on the left dot is small compared to the temperature or Γ_L and the fea-

tures in $R(\varepsilon_1, \varepsilon_2)$ merge into two horizontal bands of opposite polarity.

[29] In the model we assume a reduction of ϕ by a factor of five, corresponding to the fivefold increase of λ_{SAW} . The

correspondence between ϕ and λ_{SAW} is uniquely defined only when λ_{SAW} is larger than twice the distance between the centers of the two dots.